Quantum-confined biexcitons in CuCl quantum dots and their unconventional optical properties

2007 J. Phys.: Condens. Matter 19 445006

(http://iopscience.iop.org/0953-8984/19/44/445006)

IOP PUBLISHING JOURNAL OF PHYSICS: CONDENSED MATTER

J. Phys.: Condens. Matter **19** (2007) 445006 (21pp) doi:10.1088/0953-8984/19/44/445006

Quantum-confined biexcitons in CuCl quantum dots and their unconventional optical properties

K Miyajima, M Ashida and T Itoh

Division of Frontier Materials Science, Graduate School of Engineering Science, Osaka University, 1-3 Machikaneyama-cho, Toyonaka, Osaka 560-8531, Japan

E-mail: itoh@mp.es.osaka-u.ac.jp

Received 11 May 2007
Published 18 October 2007
Online at stacks.iop.org/JPhysCM/19/445006

Abstract

The optical properties of quantum-confined biexcitons in CuCl quantum dots (QDs) under the novel method of two-photon resonance excitation of biexcitons are reviewed. First, we briefly overview the optical properties of excitons and biexcitons in bulk CuCl single crystals and also those in quantum dots, and then we cover the biexcitonic properties of CuCl quantum dots in NaCl matrices in detail: realization of two-photon resonant excitation of confined biexcitons with different angular momenta, studies on the energy-level structure of biexcitonic states by size-selective two-photon resonant excitation of biexcitons, on subsequent efficient lasing of biexcitonic luminescence even in low-Q cavity, on ultrafast radiative decay of biexcitons, and, finally, the observation of excited states of confined biexcitons studied by infrared transient absorption. All these unconventional features are inherent in the biexcitons in CuCl QDs affected by quantum confinement effects.

1. Introduction

1.1. Exciton and biexcitons in CuCl single crystals

CuCl is an appropriate material for the study of the optical properties of the exciton and biexciton (composite particle of two excitons) because of the large exciton binding energy (effective Rydberg energy 197 meV [1]), the small exciton Bohr radius (0.68 nm) [2] and the large biexciton binding energy (32 meV for two singlet excitons in bulk crystal [3]). There are two kinds of exciton series, Z_3 and $Z_{1,2}$ excitons, separated by spin–orbit splitting. The lowest Z_3 exciton has a rather simple character because both the electron and hole states are nondegenerate except for the spin doublet. Furthermore, the excitonic polariton picture has been well established in this material [4]. See figure 1(a).

At high-density excitation of excitons, biexcitons are formed by the collision of two excitons. The most novel method for the direct creation of a biexciton is the two-photon

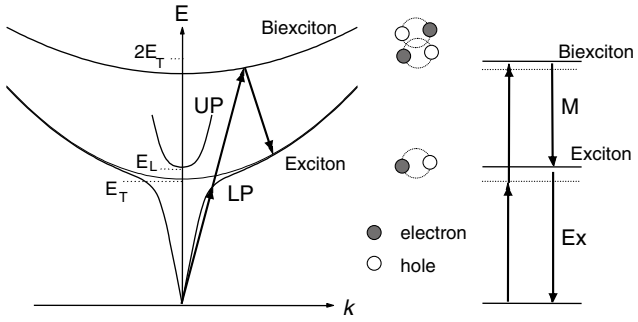

(a) bulk single crystal (b) nanocrystal

Figure 1. Schematic energy-level diagrams of exciton and biexciton systems and a schematic illustration of two-photon generation of a biexciton and its subsequent radiative decay processes. (a) For bulk single crystal, excitonic polariton dispersion is drawn, while (b) for nanocrystals, dispersionless energy levels blue-shifted by the quantum confinement effect are drawn.

absorption process of the biexciton, so-called giant two-photon absorption, as indicated by successive upward arrows in figure 1(a), which was first predicted in 1973 [5], and was first observed in bulk CuCl crystal [6]. Due to the giant oscillator strength the direct creation of a biexciton by two-photon absorption shows very large absorption coefficient compared with mid-gap two-photon absorption in bulk semiconductor crystal. The totally symmetric nature of the biexciton ground state (total angular momentum: $J = 0$) gives the polarization selection rule of CuCl bulk crystal. Linearly polarized light can create a stable biexciton, while co-circularly polarized light cannot create the $J = 0$ biexciton [7]. The $J = 2$ biexciton state is unstable due to negative binding energy.

Secondary emission of a biexciton under the giant two-photon excitation shows a peculiar nature of coexistence of hyper-Raman scattering and ordinary luminescence, as indicated by the downward arrow in figure 1(a). Together with the excitonic polariton picture, there effectively occurs a hyper-parametric scattering (in other words, polariton–polariton hyper-parametric scattering) process in which two incident photons with the same photon energy are scattered into two photons with different photon energies. This process was applied to determine the excitonic polariton dispersion curves for a wide range of wavevectors [8], and quite recently it has been successfully applied for the generation of an ultraviolet (UV) entangled photon pair from an uncorrelated incident UV photon pair [9]. The ordinary luminescence is called the M_T or M_L band, the radiative decay of biexciton leaving one transverse or longitudinal exciton behind, respectively.

The temporal behaviour of exciton and biexciton systems has also been studied mainly by picosecond spectroscopy. At low temperatures, such as liquid helium temperature, the photo-excited singlet excitons are converted into excitonic polaritons in pure crystals, and their temporal response reflects strongly the propagation dynamics of excitonic polaritons in the single crystal [4]. The longitudinal relaxation time is of the order of a few nanoseconds. On the other hand, the triplet exciton has the relaxation time of a few tens of nanoseconds. In contrast, the lifetime of a biexciton is rather short, about 70 ps, due to the giant oscillator strength for the radiative transition between biexciton and exciton states [10].

1.2. Exciton confinement in CuCl quantum dots

In KCl and NaCl crystals heavily doped with Cu^+ ions, additional absorption and luminescence bands denoted Ex similar to those of excitons in CuCl bulk single crystals appear in the

transparent energy region of pure KCl and NaCl crystals. To explain the origin of these bands, CuCl nanocrystals, in other words, quantum dots (QDs), were assumed to be formed by the coagulation of Cu^+ ions. This assumption was verified by the indirect method of small-angle x-ray scattering [11] and quite recently by direct observation in transmission electron microscopy. In semiconductor quantum dots, it is well known that three-dimensional quantum confinement of the electron, hole and exciton causes various kinds of change in the optical response. In CuCl QDs of a few nanometres in radius, quantum confinement of excitons causes mainly the restriction of exciton translational motion inside the three-dimensional quantum well with little influence on the electron–hole internal motion on account of the very small exciton Bohr radius of 0.68 nm [12]. This kind of confinement is called weak confinement (or exciton confinement); it is completely different from the strong confinement (or electron–hole individual confinement) realized in typical semiconductors, such as GaAs QDs. The exciton confinement brings about the following unconventional properties of confined excitons. With decreasing QD size, the exciton energy is shifted towards the high-energy side, as shown schematically in figure 1(b) and, in the exciton excitation spectra, the confined exciton states are split into various complicated substates reflecting the apparent discreteness of the exciton wavevectors in the band structure of the Z_3 and $Z_{1,2}$ excitons [11]. The quantum yield of the confined exciton luminescence Ex is very high, several tens of percentage. The radiative decay rate of the confined excitons increases in proportion to the QD volume on account of the complete coherence of the confined exciton wave over the crystal volume. This phenomenon is called 'exciton superradiance' [13]. As long as the exciton superradiance occurs, the size-dependent optical nonlinearities in CuCl QDs increase for larger QD sizes, the tendency of which is completely reversed compared with the optical nonlinearity of ordinary semiconductor QDs in the case of electron–hole individual confinement [14].

1.3. Biexcitons in CuCl quantum dots

The quantum confinement of biexcitons may be different from that of excitons because of the difference in their effective sizes. In CuCl QDs, a new nonlinear luminescence band M appears on the lower-energy side of the exciton luminescence Ex under the intense excitation above the exciton band. The intensity of the biexciton luminescence band M is proportional to the square of that of the exciton luminescence band Ex with the increase of the excitation power, and for QDs larger than 10 nm in radius the peak energy of the new luminescence band M nearly coincides with that of the biexciton band (M band) in the bulk crystals. (To be exact, there is some serious discrepancy in their energy positions, as discussed later.) These provide the rough evidence of the confined biexciton luminescence as the interpretation of the M band in CuCl QDs, as indicated by the downward arrow in figure 1(b). However, in contrast to the M band in bulk CuCl crystal, there is a strong tendency of saturation in the excitation power dependence of the M luminescence intensity. This fact indicates that the peculiar biexciton formation process in QDs is different from that in the bulk crystals. In the study of time-resolved pump–probe spectroscopy for the transient absorption spectra around the exciton band region under intense excitation above the exciton band, there appears induced absorption and even negative absorption (gain) at the energy region of the M band. The rise and decay kinetics of the transient absorption at the exciton Ex and biexciton M bands indicates the so-called cascade relaxation process of multi-exciton states; when multi-excitons are created in a QD, the number of excitons decreases stepwise (for example, triexciton, biexciton, single exciton and no exciton) because all the excitons are always interacting with each other due to the confinement [15]. Under the size-selective excitation inside the confined exciton band, the peak energy relation between the exciton Ex and biexciton M bands was studied [16].

However, due to the wide size distribution of the CuCl QDs, a definite interpretation was not possible. Furthermore, there has been no report concerning direct two-photon absorption into the confined biexciton state. This may give direct evidence for the origin of the M band in CuCl QDs.

In this paper, the giant two-photon excitation of confined biexcitons is experimentally observed and the subsequent unconventional optical properties of confined biexcitons have been revealed.

1.4. Experiments

CuCl QDs embedded in a NaCl matrix were prepared by the transverse Bridgman method followed by successive annealing treatment [11]. The nominal concentration of CuCl in the NaCl matrix is about 1 mol%, and the average radius ranges between 2 and 10 nm, controlled by thermal treatment. A cleaved slice of the NaCl matrix crystal was prepared and cooled down for the optical measurement. The sample temperature was kept between 4 and 77 K in a He gas flow cryostat. The sample was optically pumped by tunable laser pulses with 1 kHz repetition rate, 2 ps pulse duration and 3 meV spectral width (except for the optical Kerr gate measurement in section 2.4) generated by an optical parametric amplifier. The photoluminescence (PL) was collected in forward-scattering geometry except when otherwise specified, and the spectrum was detected by using a spectrometer equipped with a liquid nitrogen cooled charge-coupled device (CCD) array. For time-resolved transient absorption spectra, the pump–probe method was adopted, and for the sub-picosecond time-resolved luminescence spectra, the optical Kerr gate method was used. The details of the experimental methods other than those described here will be given more in detail in the corresponding sections.

2. Biexcitonic properties in CuCl quantum dots in NaCl matrix

2.1. Two-photon resonant absorption of biexcitons

We observed and verified the two-photon absorption band of the biexcitons in the CuCl QDs by using the polarization selection rule. In addition, we found the two-photon absorption of the excited biexciton with $J = 2$, which has a large transition dipole moment for the transition from the exciton state of $J_{ex} = 1$ in the QD [17].

Figure 2 shows photoluminescence (PL) spectra with the excitation energy of 3.228 eV (thick line) and 3.184 eV (thin line), respectively, together with the absorption spectrum (dotted line) at 4 K. The photon energy of 3.228 eV corresponds to the resonant excitation of the confined excitons. The PL bands denoted by M, BM, BX and I_1 originate from free biexcitons, bound biexcitons, bound excitons and I_1 bound excitons, respectively [18]. On the other hand, in the case of the excitation energy of 3.184 eV, which is lower than the lowest-energy edge of the absorption band, the PL bands of M, BM and BX were also observed. In this excitation condition, the excitons are not created by the one-photon absorption process. The biexcitons are created through two-photon excitation, as shown in figure 1(b).

Figure 3 shows PL excitation (PLE) spectra of the M and BM bands with the linearly polarized (a) and circularly polarized (b) excitation light, respectively. For the linearly polarized excitation, the PLE spectrum has a peak around 3.21 eV with a broad high-energy tail. In addition, the PLE intensity decreases monotonically towards the lower-energy side. The isolated peak structure due to the resonant two-photon absorption process, which was clearly observed in the bulk crystal [6], was not observed, because of the inhomogeneous size distribution of the dots. On the other hand, for circularly polarized excitation, the PL intensities

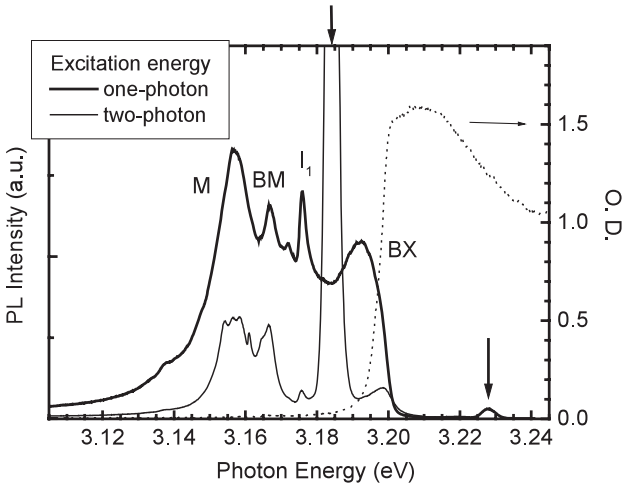

Figure 2. PL spectra of CuCl QDs at 4 K with excitation energies of 3.184 eV (thin curve) and 3.228 eV (thick curve), respectively. The one-photon absorption spectrum is also shown as a dotted curve. Arrows show the excitation energy positions.

of the M and BM band decrease abruptly below 3.204 eV. This value almost coincides with the transverse exciton energy in bulk crystal, 3.202 eV.

The polarization dependence of the PLE for the excitation light can be seen more explicitly by plotting the ratio of the PLE spectra, as shown in figure 4. The ratio spectrum was obtained by dividing the PLE intensity under the circularly polarized excitation by that under the linearly polarized excitation. When the excitation photon energy is lower than 3.204 eV, the PL intensities of the M and BM bands decrease for the circularly polarized case compared to the linearly polarized one. This feature of the PLE agrees with the polarization selection rule for the lowest biexciton ($J = 0$). Therefore, this is clear evidence for the existence of the direct creation process of the lowest biexciton confined in CuCl QDs by two-photon absorption.

On the other hand, the ratio exceeds unity at an excitation photon energy higher than 3.204 eV. This means that the biexcitons are created more efficiently with the circularly polarized light than with the linearly polarized one. In order to explain this polarization dependence, we assumed the resonant two-photon absorption of the excited biexciton states, the energies of which are larger than twice the creation energy of the isolated excitons [19, 20]. According to the previous report [19], two of the excited biexciton states ($J = 0$; 2) are optically allowed for the transition from the exciton state with $J_{ex} = 1$; and the transition dipole moment for the $J = 2$ biexciton state is much larger than that for $J = 0$ biexciton state. For the two-photon absorption process of the biexciton, the giant transition dipole moment between the exciton and biexciton enhances the two-photon absorption coefficient. Under this assumption, it is reasonable to consider that resonant two-photon absorption for the excited biexciton of $J = 2$ has a larger dipole moment than that for $J = 0$. Consequently, the polarization dependence of the PLE above 3.204 eV can be explained.

When the excitation energy is lower than the one-photon absorption band of the excitons, the lowest biexcitons are created directly by two-photon absorption. On the other hand, when the excitation energy falls into the absorption band of the excitons, the biexcitons are created into the excited state, and then relax into the lowest state.

In summary, by the polarization dependence of the PLE spectra of the biexciton on the excitation light, we clarify the existence of the two-photon absorption process of the lowest

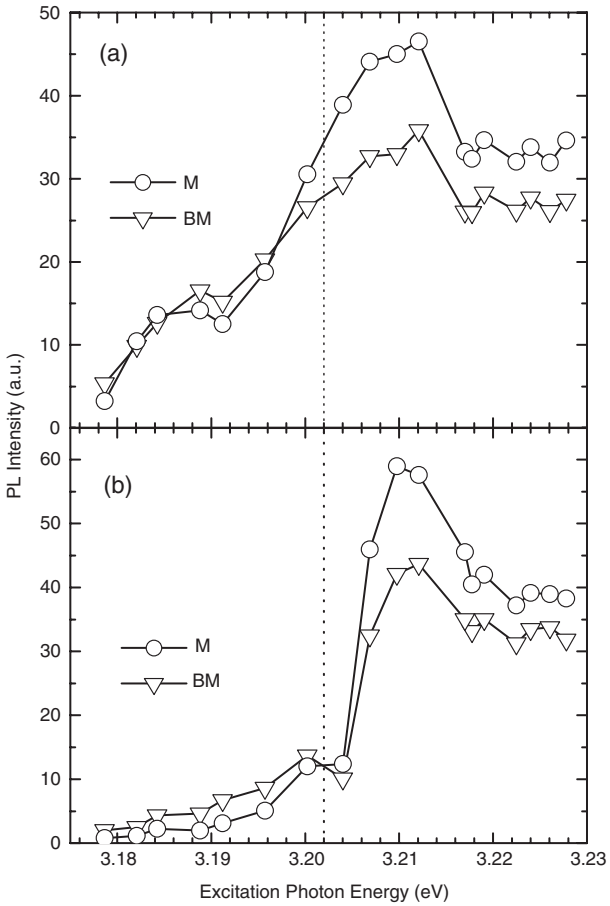

Figure 3. PLE spectra of the M band (open circle) and BM band (open triangle) at 4 K with the linearly polarized (a) and circularly polarized (b) excitation light.

biexciton. Furthermore, we found the two-photon absorption process of the excited biexciton state, which becomes stable in the QDs. The two-photon excitation method is very useful for the study of the physical properties of biexcitons confined in the QDs, as demonstrated below.

2.2. Size-selective excitation of biexcitons under two-photon resonant excitation

Fine-energy structures hidden in inhomogeneous broadening of exciton levels of QDs with large size distribution can be revealed by size-selective excitation; tuning the excitation photon energy gives rise to the dot-size dependence of the exciton properties. However, in the case of size-selective exciton band excitation, successive absorption of two photons having the exciton energies would not generate biexcitons in the QDs, because the second exciton should be generated with somewhat different photon energy from that required for the first exciton due to the mutual correlation between the two excitons. Previous methods for the investigation of biexciton energy in CuCl QDs were performed using the following two methods: (1) PL energy under the resonant excitation of higher confinement states of the exciton [16], and (2) the peak energy of photo-induced absorption for the transition from the exciton to the biexciton states [20]. However, the reported size dependences were different for radii smaller

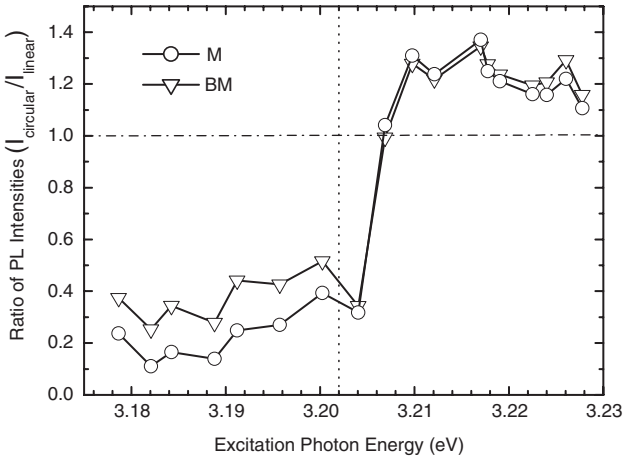

Figure 4. Ratios of the PLE spectra of M band (open circle) and BM band (open triangle), respectively. The ratio was calculated by dividing the PLE intensity under the circularly polarized excitation by that under the linearly polarized one.

than ∼3 nm: the reason for this has not been clarified so far. In addition, the stepwise process of generating the biexcitons via the real state of the excitons using two beams is rather complicated, and its interpretation is not straightforward due to the relaxation processes during the generation of the biexcitons.

Here we describe the size-selective excitation of biexcitons using direct two-photon resonant excitation [21]. Until now, two-photon resonant excitation of the biexcitons in the quantum structure has been used to identify biexciton luminescence in QDs and to clarify the biexciton binding energy [22–24]. In addition, since there is no excess energy corresponding to the stabilization energy that binds two excitons in the process of generating the biexcitons, the generation and cascade relaxation processes of the biexcitons and excitons can be considered rather simply. The PL of the free excitons could not be observed at low temperatures since the bound exciton PL was dominant. Therefore, we measured the PL spectra at higher temperatures to confirm the size-selective excitation of the biexcitons by observing the PL of the free excitons.

Figure 5(a) shows the PL spectrum (excitation using a continuous-wave (cw) HeCd laser with a wavelength of 325 nm) and the absorption spectrum at 77 K denoted by solid and dashed lines, respectively. The excitation wavelength corresponds to the band-to-band excitation of CuCl. For the PL peak energy of 3.229 eV, the average dot radius was estimated to be 3.6 nm. The spectral width was ∼17 meV, which corresponds to a size distribution ranging from 5.2 to 2.8 nm.

Figure 5(b) shows the PL spectra for different excitation photon energies of the tunable light source at the lower-energy side of the exciton band. The PL band of the biexcitons was observed at the lower-energy side of the scattered excitation light, as indicated by the downward arrow. The biexciton luminescence has two peaks (or shoulders), which are denoted by M and BM. In the previous report on the PL spectra under the high-density excitation of the excitons, it was suggested that the M and BM bands were attributed to the free and bound biexciton states, respectively [18]. In addition, the additional PL band with the broader spectral width seems to overlap with these peaks, and its peak energy shifts to the lower-energy side as the excitation photon energy decreases. Although this new band might be a biexciton band size-selectively excited by the two-photon resonant excitation, it is difficult to derive the entire shape of this PL

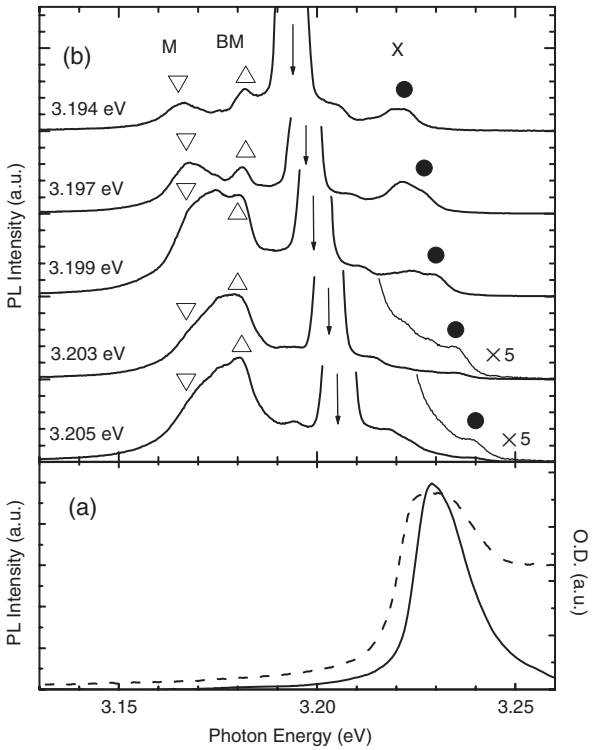

Figure 5. (a) PL spectrum (solid curve) under a cw HeCd laser (325 nm) excitation, and absorption spectrum (dashed curve) of CuCl QDs at 77 K. (b) PL spectra under the resonant two-photon excitation of biexcitons at 70 K for different excitation photon energies indicated by downward arrows, which are also shown on the left-hand side of the spectra. The peaks or shoulders for the M and BM bands are denoted by inverted triangles and open triangles, respectively. The peaks for the X band are denoted by closed circles. The enlarged spectra of the X bands at the excitation energies of 3.205 and 3.202 eV are also shown.

band from the obtained spectra because the PL spectral structures are rather complicated. On the other hand, at the higher-energy side of the excitation photon energy, the PL band (denoted as X) was observed: its peak energy decreased with the excitation photon energy. The X band is attributed to the confined free excitons because its peak energy is located inside the exciton band shown in figure 5(a). Since the excitons are not directly generated by the excitation light under these excitation photon energies, the excitons are generated during the radiative relaxation of the biexcitons generated by the two-photon resonant excitation. Since the PL intensities of both the X and M bands exhibited nearly quadratic dependences ($I_{exc}^{1.7}$) on the excitation intensity I_{exc}, we conclude that the biexcitons and excitons are selectively generated in the specific dot size chosen for the two-photon resonant excitation of the biexcitons.

Here, it is important that the dot radius excited by the two-photon excitation of the biexcitons can be derived from the PL energy of the excitons. Since the large size distribution induces resonant excitation not only in the lowest state but also in the higher confinement states of the biexcitons, more than one peak is observed in the X band under certain excitation photon energies. In addition, the relative intensities of some peaks in the X band are influenced by the distribution of the dot radius in the sample. Therefore, we focus on the highest-energy peak (denoted by solid circles in the X band) for the analysis of the size dependence on the generation

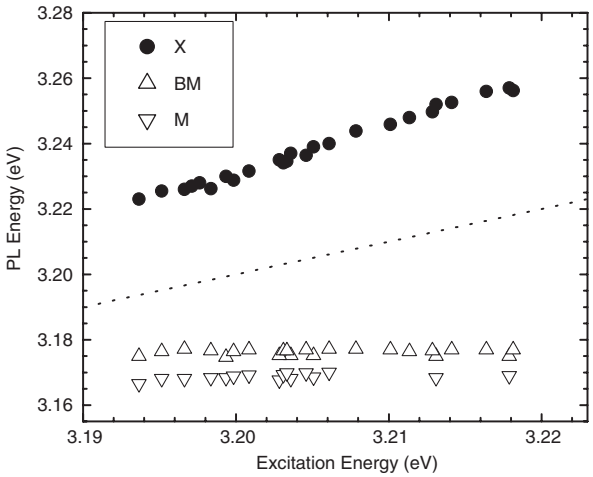

Figure 6. Excitation photon energy dependences of the PL peak energy of the X band (closed circles) and the BM and M bands (open triangles and inverted triangles, respectively). The dashed line indicates the excitation photon energy for the two-photon resonance.

of the biexcitons under the assumption that the excitation of the lowest state of the biexciton yields the highest energy for the excitons following the radiative decay of the biexciton, even when the lower-energy peak is stronger than the higher-energy one. The PL photon energies of the M, BM, and X bands are plotted as functions of the excitation photon energy in figure 6.

The PL energy of the M and BM bands are almost constant, but that of the X band varied sensitively with the excitation photon energy. Under the two-photon excitation of the biexcitons, the excitation photon energy should be located just in the middle between the biexciton and exciton PL energies. However, the experimental result did not agree with this relationship. Therefore, we examined two types of method to analyse the transition energy between the biexciton and exciton states.

First, we focused on the PL peak energies of the M bands. The PL energy of the M band under two-photon resonant excitation coincides with that under band-to-band excitation [16]. On the other hand, when we compare the PL energy of the M and BM bands with that under the size-selective excitation of the excited exciton states, they do not agree even though the size-selective excitation of biexcitons has been employed [16]. However, the M and BM bands under the two-photon resonant excitation are superimposed with the third PL band—the photon energy of this band depends on the excitation energy. These results imply that the radiative transition process from the biexciton to exciton states contains an additional unknown biexciton state, other than those states related with the M and BM bands.

Next, we analyse the transition energies between the biexciton and exciton states according to the relationship between the excitation photon energy (E_{exc}) and the exciton PL energy (E_x): $2E_{\mathrm{exc}} - E_x$, assuming ideal two-photon resonant excitation. The calculated transition energy after calibrating for 77 K is plotted in figure 7, together with the photo-induced absorption energy for the transition from the exciton to biexciton states, which was reported in [20]. These results agree well with each other. This indicates that a common biexciton state exists for both two-photon resonant excitation and induced absorption. Furthermore, the discrepancy with the M band energies indicates that the biexciton state yielding the M band is different from the biexciton state directly excited by the two-photon resonant excitation.

When the intrinsic states of the biexcitons and excitons are considered, several confinement modes other than the lowest states of the biexcitons and excitons should be related to the

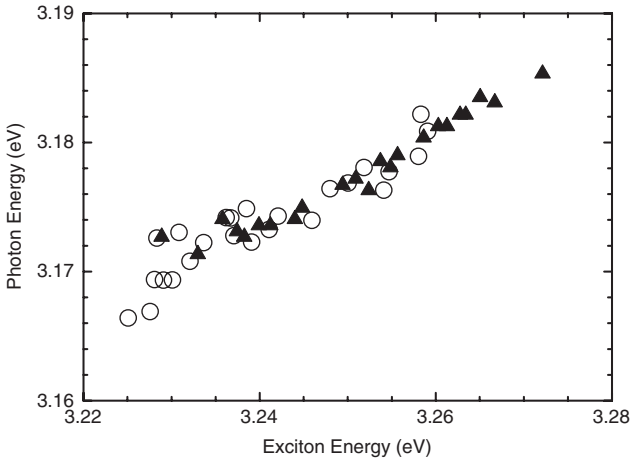

Figure 7. Comparison of the calculated transition energy (open circles) between the biexciton and exciton states under the two-photon resonant excitation with induced absorption energy (closed triangles) for the transition from the exciton to biexciton states reported in [20].

transition process. For example, a report suggests that the exciton in the weak confinement regime exhibits L–T mixed modes and the surface mode [25], which might be the final exciton states for the M band transition. However, the biexciton states under the two-photon resonant excitation are considered to be the lowest state with $J = 0$. In addition, it is well known that the observed exciton PL is due to the lowest state of the free exciton. Since the PL energy of the M band is lower than the expected transition energy, it can be reasonably suggested that the free biexciton directly generated by the two-photon resonant excitation rapidly relaxes to a certain bound state, for example, the surface modes. On the other hand, there is a possibility that the final state of the exciton is not the lowest state but the excited state of the quantum confinement levels. However, the oscillator strength of the transition between the lowest states of the biexcitons and excitons is considered to be the strongest in comparison to the other transitions related to their higher excited states of the quantum confinement levels. Therefore, it is reasonable to suggest the former case, although the transition dynamics and the energy levels for biexcitons and excitons in the CuCl QDs need to be discussed further. Consequently, we conclude that two-photon resonant excitation is quite useful to evaluate the size dependence of the biexciton properties for samples having large dot-size distributions.

2.3. Biexciton lasing under exciton excitation and under two-photon resonant excitation

In the first subsection, we have described the two-photon resonant excitation of the biexcitons in CuCl QDs. On increasing the excitation intensity under the two-photon absorption of biexcitons, we have found stable and low-threshold laser emission [26, 27].

PL spectra of CuCl QDs measured under the resonant two-photon absorption at 4 K are shown in figure 8. The excitation energy is 3.195 eV, as indicated by arrow, which is about 10 meV below the one-photon resonance for the confined excitons of 7 nm QDs. At a pumping intensity of $1.0I_{\mathrm{th}}$, the spectrum consists of three luminescence bands, marked with M, BM and I_1, which are luminescence bands, respectively, associated with the free biexciton, the surface-bound biexciton typical for QDs, and the I_1 bound exciton common both for bulk and nanocrystals [18]. On increasing the pumping intensity, intense multiple mode peaks appear

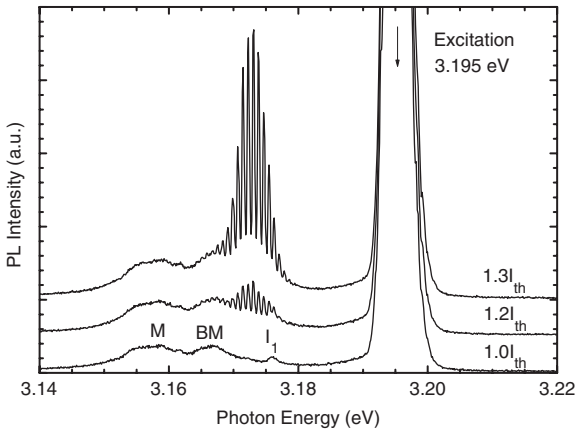

Figure 8. Luminescence spectra (solid line) of CuCl QDs under the two-photon resonant excitation of biexcitons at 4 K. The arrow indicates the two-photon excitation energy. M, BM and I_1 denote free biexciton, bound biexciton and bound exciton luminescence, respectively. The laser action appears around the BM band.

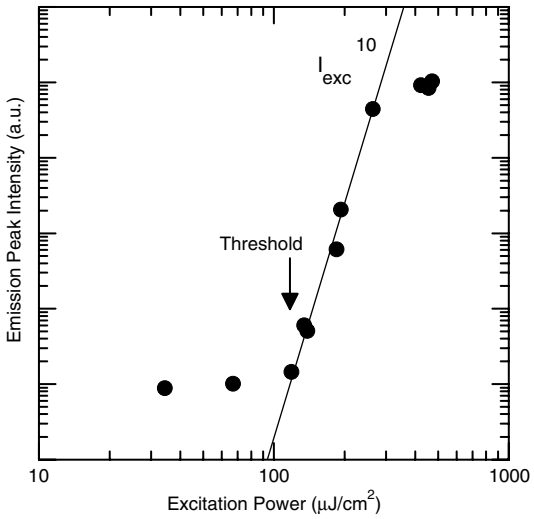

Figure 9. Peak intensity dependence on excitation power. The laser threshold is estimated to be 120 μJ cm^{-2}.

near the BM band. The emission peak intensity is plotted against the excitation intensity in figure 9. As seen in the figure, the threshold of the lasing is 120 μJ cm^{-2}.

Next, we examined the polarization dependence of the laser emission for the pump light in order to confirm that it originates from biexciton states. Since the lowest state of the biexciton in CuCl has a total angular momentum of $J = 0$, biexcitons cannot be created with co-circularly polarized light for the two-photon absorption process, as shown in the previous section. Figure 10 shows PL spectra with linearly and circularly polarized pump light with the excitation intensity of 0.47 mJ cm^{-2}. Circularly polarized light was produced by a quarter waveplate. The lasing mode was observed with linearly polarized pump light; however, it

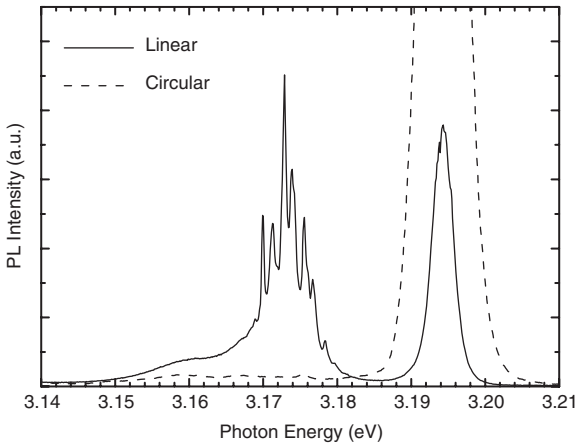

Figure 10. PL spectra with linearly (solid) and circularly polarized (dashed) pump light.

disappeared with circularly polarized pump light. As a result, we confirmed that the biexciton state, which is excited directly by the pump laser, causes laser emission.

Above the threshold, we observed multilines due to the lasing mode by optical amplification inside the sample. The direction of the observed laser emission was normal to the sample surfaces. This fact indicates that optical amplification is provided by sample surfaces acting as an optical cavity. In order to confirm this amplification mechanism, we investigated the relation between the lasing mode distance (D_n) and sample thickness. An optical resonator satisfies the relation $D_n = c/2nl$, where c is the speed of light in vacuum, n is a refractive index of the medium and l is the cavity length. Figure 11 shows laser emission spectra of three samples with thicknesses of (a) 0.48 mm, (b) 0.32 mm and (c) 0.29 mm. By decreasing the sample thickness, the average mode distance increased and the values are obtained as (a) 1.98×10^{11} s^{-1}, (b) 2.94×10^{11} s^{-1} and (c) 3.22×10^{11} s^{-1}. Using the above relation with $n = 1.59$ for NaCl, the cavity lengths are calculated to be 0.46, 0.30 and 0.27 mm, respectively. The calculated cavity lengths coincide with sample thicknesses. From these results, we confirmed that the optical feedback for lasing is provided by the reflection at the NaCl crystal surfaces, where their reflectivity is only about 6%. The laser action was stable over several tens of minutes and could be observed up to 70 K, but it depended on the position of excitation on the sample surface because of the low Q-factor.

Figure 12 shows PL spectra under one-photon absorption into the exciton state at 4 K. The excitation energy is 3.228 eV. At weak excitation conditions, a BX band associated with a surface bound exciton typical for nanocrystals additionally appears around 3.195 eV. At high pumping intensity such as a few mJ cm^{-2}, the lasing of biexcitons is also observed at some parts of the sample.

In the case of lasing under the one-photon absorption of the excitons, the laser action was found to damp within a few seconds just after the start of the lasing, as shown in figure 13. Figure 14 shows the comparison of the temporal changes of lasing intensity between the one-photon and two-photon excitation conditions. The laser action under the two-photon excitation condition showed high stability, while for the one-photon excitation condition the lasing is unstable, and had a very short life time.

The observation of light amplification has been reported for CdSe [28, 29], CuCl [30], Si [31] and PbSe [32] nanocrystals. However, these demonstrations have been carried out by one-photon interband excitation. In QDs, carriers and excitons are confined within all three

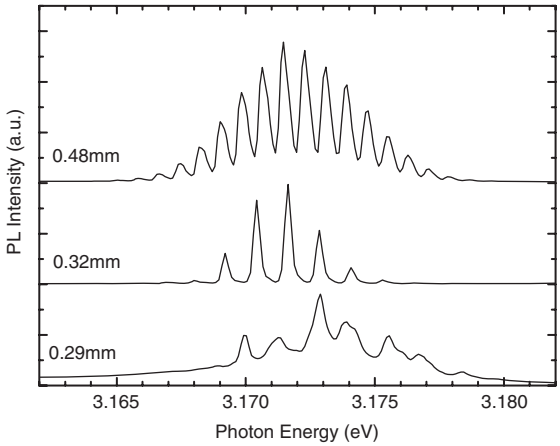

Figure 11. Enlarged spectra of multimode laser action of three samples with thicknesses 0.48 mm, 0.32 mm and 0.29 mm, respectively.

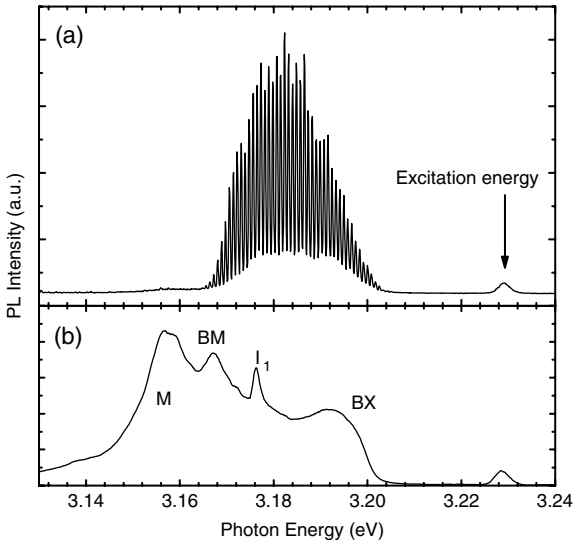

Figure 12. PL spectra under one-photon absorption into the exciton state at 4 K above the threshold power density of about 1 mJ cm^{-2} (a) and in the weak excitation condition (b). The arrow shows the excitation energy position.

dimensions, and radiative recombination processes are in great competition with the efficient nonradiative Auger process [33]. Because of the high loss due to the efficient nonradiative process, lasing was generally achieved only with the help of a high-Q feedback system. However, in our case of resonant two-photon excitation, the lasing threshold was lower than that in the earlier report [30] in spite of the low-Q cavity. This implies that lasing under two-photon absorption shows a drastic improvement of the efficiency of light amplification.

In semiconductor QDs, the optical gain is attained when the number of biexcitons is dominant over that of excitons [6, 30]. If only one biexciton is directly created in a QD, a complete population inversion is realized straightforwardly. Therefore, the two-photon resonant excitation of biexcitons should bring about a stable and efficient lasing process. In

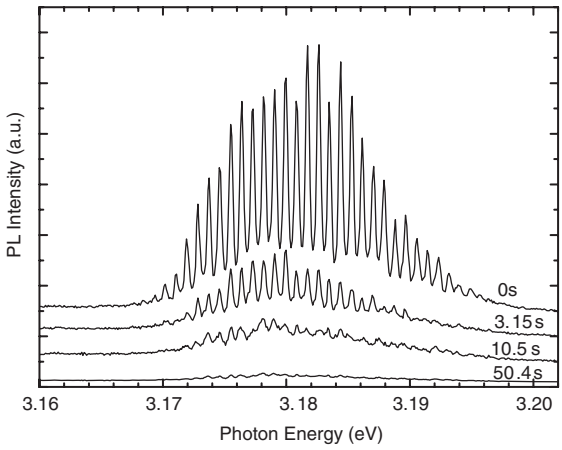

Figure 13. Temporal change of laser spectra under one-photon excitation.

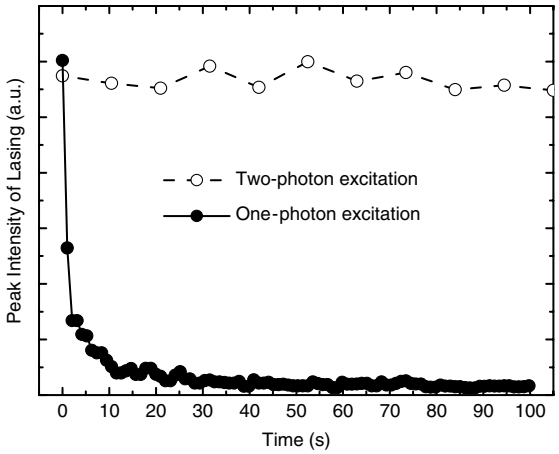

Figure 14. Comparison of temporal changes of laser intensity between the one-photon (closed circles) and two-photon (open circles) excitation conditions.

contrast, a rapid damping was observed in the case of intense one-photon excitation, since the interaction of unbound multiexcitons causes efficient Auger ionization of QDs. The direct generation process of biexcitons by two-photon resonant excitation effectively suppresses the Auger recombination process without the participation of unbound excitons.

2.4. Rapid radiative decay of biexcitons under two-photon excitation

By means of ultrafast time-resolved spectroscopy with the use of an optical Kerr gate method, we found a new PL band, which emerges in an ultrashort stage only under resonant two-photon excitation conditions. Here we suggest that this PL band gives rise to the laser emission described in the previous subsection [34].

For the optical Kerr gate measurement, Ti:sapphire laser light after regenerative amplification (pulse width of 220 fs, wavelength of 800 nm, repetition rate of 1 kHz) is split into two beams. One is used to pump an optical parametric amplifier (OPA). The excitation

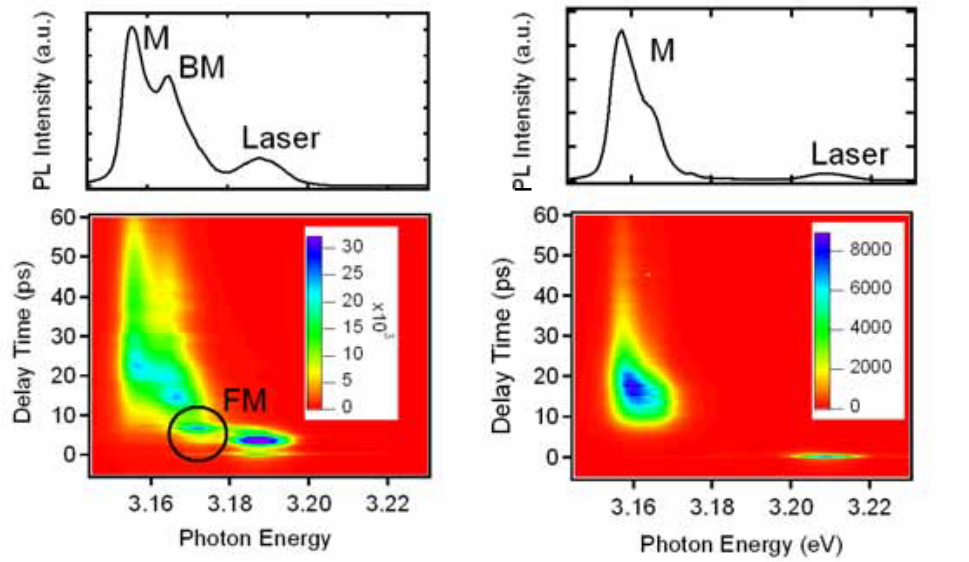

Figure 15. PL spectra and the time-resolved PL images at 4 K under the resonant excitation of the resonant two-photon excitation of the biexciton (left) and the resonant excitation of the exciton (right). The circle indicates the position of a new emission FM band.

(This figure is in colour only in the electronic version)

pulse was obtained from a fourth-harmonic generation using two beta barium borate crystals from a signal beam from the OPA. Another pulse is used for the gate pulse. The Kerr medium was toluene, and the time resolution was about 1 ps. The excitation pulse was irradiated on the sample with a pencil-shape volume with the length of 800 μm through a cylindrical lens. The PL from an edge of the sample was collected and detected with a combination of a spectrometer and a CCD.

The time-integrated PL spectra and the time-resolved PL images under the resonant excitation of the exciton (the excitation energy of 3.209 eV) and the resonant two-photon excitation of the biexcitons (3.192 eV) are shown in figure 15. The excitation intensities were 2.3 and 3.8 mJ cm^{-2}, respectively. In the case of the resonant excitation of the excitons, the M band is dominant. The PL due to the exciton or bound exciton states is not observed, because of the effective reabsorption process in the sample. The PL intensity of the M band reached a maximum at the delay time of 20 ps, and decayed rapidly with the time constant of 11 ps. Under two-photon excitation, on the other hand, the M and BM at bands are observed separately. The delay times to their maxima were 20 and 11 ps, respectively, and their decay times were about 40 ps. In addition, a new PL band denoted by FM at 3.173 eV emerged before the rise of the BM band. In a previous report on the biexciton dynamics under the band-to-band excitation, the rise times of the BM and M band were less than 2 ps, and the decay time of the M band was 120 ps [18]. However, the rise and decay times obtained in this measurement were quite different. For the rise times, the propagation time of the emission seems to be effective. However, the excitation length of 800 μm corresponds to the delay time of $\sim$4 ps by considering the refractive index of the NaCl matrix ($n = \sim 1.5$). Consequently, this effect is small.

We suggest that the slow rise times may be attributed to the transition dynamics from two excitons to a biexciton: The present case is the resonant excitation of the exciton, while the

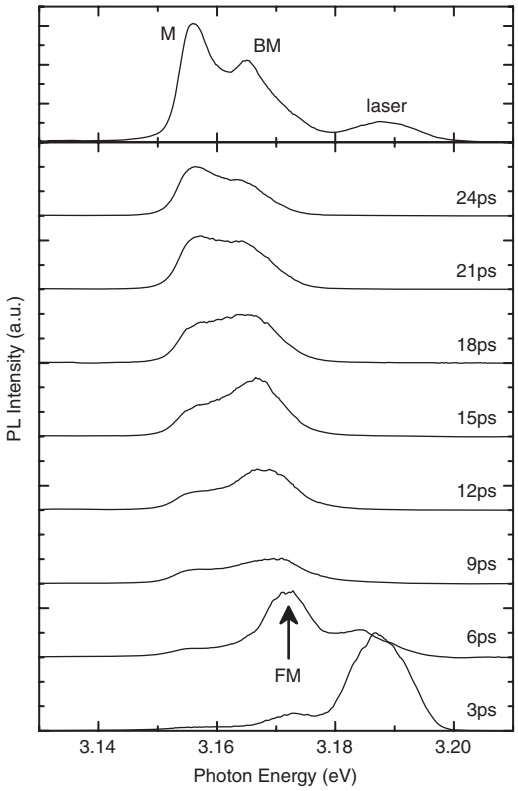

Figure 16. Time-resolved spectra with delay times extracted from figure 15 and a time-integrated spectrum (uppermost) under the resonant two-photon excitation of the biexciton. The arrow indicates the position of a new PL band denoted FM.

case of [18] is the band-to-band excitation. The excitation density may also affect the rise time due to the Auger process. However, in the case of two-photon resonant excitation, it is expected that the delay times should be very short because the biexciton is generated directly. The unexpectedly long delay time for the M band suggests that the initial state for the M band cannot be the biexcition state which is resonantly excited, as already discussed in section 2.2. Furthermore, the most characteristic feature of the two-photon excitation is the appearance of the new PL band. Figure 16 shows the PL spectra with some delay times and the time-integrated spectrum extracted from figure 15. The FM band was observed clearly at the delay time of 6 ps, although it was not seen in the time-integrated PL spectrum. Since this band disappeared under the circularly polarized excitation pulse, we conclude that this FM band is caused by the biexciton state. Assuming that the M band is not due to the free biexciton but due to the biexciton trapped to the shallow impurity, we can say that the FM band originates from the *free biexciton state*. On the other hand, the temporal profile with the pulse-like shape of the FM band is very interesting. This non-exponential decay behaviour strongly suggests the occurrence of *superfluorescence* predicted by Dicke [35]. Details will be reported elsewhere. Finally, we discuss the possibility that FM band is the origin of the laser emission. By comparing the photon energy of the lasing in figure 8 in section 2.3 and that of the FM band in figure 16, they are seen to be almost consistent. In addition, the PL intensity increases superlinearly with the excitation intensity, which indicates that this PL is amplified with the high optical

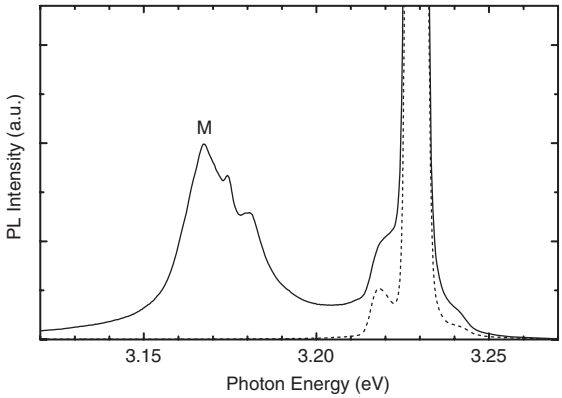

Figure 17. PL spectrum under excitation at 3.227 eV at 70 K. Scattered excitation light is also shown (the dotted curve). The biexciton luminescence (M) is observed.

gains. From these results, it is strongly suggested that the laser emission originates from the FM band under two-photon excitation. In the previous subsection, where the excitation pulse has narrower spectral width (∼3 meV), the lasing photon energy changed very sensitively to the excitation photon energy, although the BM and M bands were almost independent. In this experiment, the large spectral width of the excitation light prevents us observing the variation of the PL photon energy. It is necessary to measure the temporal profiles of the PL spectra with an excitation pulse of narrow spectral width in order to expose the biexciton transition process and its nonlinearity in CuCl QDs.

2.5. Biexciton excited state studied by infrared transient absorption

Infrared transient absorption (IRTA) measurement under the excitation of the lowest excited state of a material provides the energy structures of the higher excited states. Here we apply this method and discuss the characteristic nature of the excited states of the excitons and biexcitons confined in the QDs [36].

Optical pulses for the IRTA measurements were provided by a dual optical parametric amplifier (OPA) system pumped by an amplified mode-locked Ti:sapphire laser. The pump pulse was obtained by the fourth-harmonic generation of the signal beam of one OPA, and the wavelength was tuned to 384.1 nm, which corresponds to the resonant excitation of an exciton confined in the QDs with the effective radius ∼4.2 nm. The pump pulse (maximum energy of 8 μJ) was focused on the sample with a spot size of ∼300 μm. The probe pulse was generated from the idler beam (2.1–2.9 μm) or difference frequency generation of the signal and idler beams (3.3–9 μm) of the other OPA. The probe pulse transmitted from the sample was detected with a HgCdTe detector. The spectral resolution was ∼3 meV, which was limited by the spectral width of the probe pulse.

The PL spectrum obtained under the excitation intensity of 2 mJ cm^{-2} is shown in figure 17. The resonant PL from the exciton is not distinguishable from the scattered excitation light at 3.227 eV shown by a dotted line. The M band, which appears in the lower-energy side of the excitation light, is due to the radiative de-excitation from the biexciton state to the exciton state. Thus, it is evident that biexcitons were created in a considerable amount of QDs under this excitation condition.

Figure 18 shows the temporal profile of the IRTA measured at a probe photon energy of 250 meV under an excitation intensity ∼2 mJ cm^{-2}. The temporal profile of the IRTA

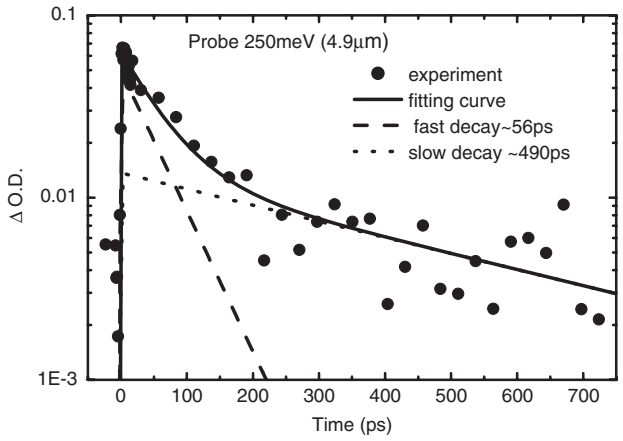

Figure 18. Temporal profile of the IRTA measured at a probe photon energy of 250 meV. The excitation condition is the same as in figure 17. The solid curve is fitted to the data assuming two decay components (56 and 490 ps).

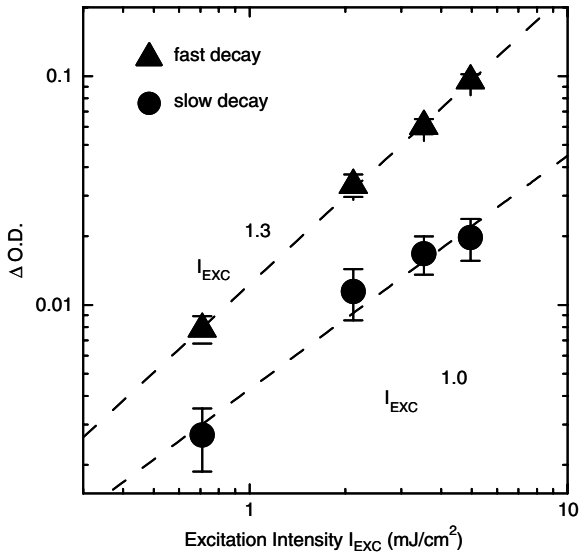

Figure 19. Excitation intensity dependences of the initial height of the two decay components: fast component (closed triangles) and slow component (closed circles).

exhibits two decay components. The faster decay time (τ_1) is $\sim$56 $\pm$ 15 ps and the slower one (τ_2) is $\sim$490 $\pm$ 290 ps. These decay times are almost the same as the previously reported lifetimes of the biexciton ($\sim$65 ps) and exciton ($\sim$380 ps) in the QD, respectively. Figure 19 shows the excitation intensity dependences of the initial height (at $t = 0$) of the two decay components. The faster decay component increases superlinearly ($I_{exc}^{1.3}$) with the excitation intensity, while the slower one has a linear dependence ($I_{exc}^{1.0}$). From these results, we conclude that the transient absorption with faster and slower decay times is induced from the confined biexciton and exciton states, respectively.

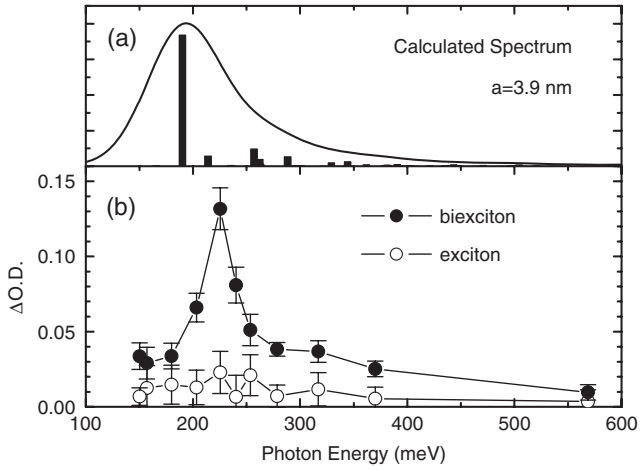

Figure 20. (a) Theoretical IRTA spectrum due to an exciton confined in QDs with the effective radius ∼3.9 nm [37, 38]. (b) The IRTA spectra due to the biexciton (closed circles) and the exciton (open circles).

Figure 20(b) presents the IRTA spectra originating from the biexciton and the exciton. The transient absorption is almost dominated by the biexciton absorption at this excitation intensity (∼2 mJ cm^{-2}). The absorption spectrum has a main peak at 225 meV (spectral width ∼50 meV) with a tail to the higher-energy side. On the other hand, in the absorption spectrum of the exciton, we could not observe any structures because of the insufficient signal to noise ratio. In the following, we focus on the IRTA from the confined biexciton state in comparison with that due to the confined exciton discussed in previous reports [37–39].

For an exciton confined in spherical QDs, the transition energies from the lowest (1S, 1s) state to the P-like states (nP, n′s), (nS, n′p), etc, have been calculated [37, 38]. Here, the notation (X, y) indicates that the state belongs to the Rydberg quantum state of X and the confinement quantum state of y. A theoretical IRTA spectrum of CuCl QDs with the effective radius $a^* = 3.9$ nm is shown in figure 20(a) [37, 38]. The vertical lines indicate the transition energies and strengths of the P-like states. The continuous spectrum was obtained by convoluting the line spectrum with a Gaussian function with an arbitrary width (∼40 meV). It has a main peak at 190 meV that originates from the transition to the (2P, 1s) state, and several small peaks due to (nP, 1s) ($n > 2$) and others on the higher-energy side. The observed spectral shape of the transient absorption from the biexciton is quite similar to the calculated spectrum for the confined exciton, although the dot size is slightly different. The calculated transition energy to the (2P, 1s) state as a function of the dot size is plotted by the solid curve in figure 21, together with our experimental value (closed diamond), the experimental data for the exciton from [39] (open circles), and that for bulk crystals [1] (dashed line). The peak energy of the IRTA for the excitons and biexcitons confined in CuCl QDs almost coincides with the transition energy of the 1S–2P state of the confined exciton. Also, the spectral shape of the IRTA has a wide tail on the higher-energy side, implying the absorption to the higher excited states.

In order to explain the obtained results, we consider the following assumption. The lowest state of the biexciton is composed of two 1S excitons. The excited biexciton states are composed of one 1S lowest exciton and one excited exciton (e.g. 2P state). In general, such states would not be stable in bulk crystals and the biexciton would separate into the two excitons, since the excess energy of the excited state is considerably larger than the biexciton

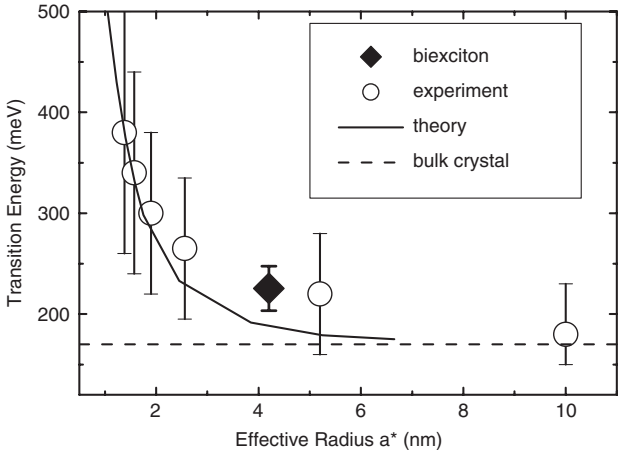

Figure 21. QD size dependence of the IRTA peak energy. The open and closed circles indicate the IRTA peak energies due to the exciton and the biexciton (the present result), respectively. The solid line indicates the theoretical transition energy from 1S to 2P exciton states. The broken line indicates that for the bulk crystal [39].

binding energy (∼50 meV). In 3D confinement, as in the case of QDs, however, the two excitons do not separate, so the excited biexciton states are stable. Under this assumption, it is reasonable that the observed IRTA spectrum of the biexciton is very similar to that of the exciton. In addition, it is interesting that the observed IRTA from the biexciton state is much stronger than that of the exciton. Taking account of the fact that after the decay of one biexciton there remains one exciton, we suppose that the absorption cross section of the biexciton is more than twice as large as that of the exciton (giant oscillator strength). Furthermore, in order to interpret the observed results and to obtain a quantitative concept, a theoretical calculation of the excited states of the confined biexciton should be performed.

In conclusion, we found two decay components of the IRTA attributed to the confined exciton and biexciton states. The IRTA of the biexciton shows a similar spectrum to that of the confined excitons. From these results, the excited biexciton states are not much different from those composed of one exciton in the lowest state and the other in the excited states. Our results experimentally establish a new understanding of the excited states of the confined biexciton and multiexciton states. The measurement on the IRTA under the resonant two-photon excitation of biexcitons is under way. The results will be reported in the near future.

3. Summary

Size-dependent optical properties of confined biexcitons were investigated in CuCl QDs, and various kinds of unconventional optical properties inherent in the quantum confinement have been revealed, especially under the two-photon resonant excitation of confined biexcitons. The quantum dots of CuCl are found to have high potentiality not only as an ideal typical material for the fundamental study on weak confinement effects on exciton and biexciton systems, but also as a laser medium or an ultrafast optical nonlinear material, especially under the condition of direct generation of biexcitons by two-photon absorption. Further study is in progress to clarify these features in more detail.

Acknowledgments

This work was supported by the 21st Century COE program (G 18) by the Japan Society for the Promotion of Science and also partially by CREST (Core Research for Evolutional Science and Technology) from the Japan Science and Technology Agency.

References

[1] Saito K, Hasuo M, Hatano T and Nagasawa N 1995 *Solid State Commun.* **94** 33
[2] Nikitine S 1962 *Prog. Semicond.* **6** 235
[3] Itoh T, Katohno T and Ueta M 1984 *J. Phys. Soc. Japan* **53** 844
[4] Ikehara T and Itoh T 1991 *Phys. Rev.* **44** 9283
[5] Hanamura E 1973 *Solid State Commun.* **12** 951
[6] Gale G M and Mysyrowicz A 1974 *Phys. Rev. Lett.* **32** 727
[7] Hanamura E 1975 *J. Phys. Soc. Japan* **39** 1516
Nagasawa N, Mita T and Ueta M 1978 *J. Phys. Soc. Japan* **45** 713
[8] Itoh T, Suzuki T and Ueta M 1977 *J. Phys. Soc. Japan* **42** 1069
[9] Edamatsu K, Oohata G, Shimizu R and Itoh T 2004 *Nature* **431** 167
[10] Ikehara T and Itoh T 1991 *Solid State Commun.* **79** 755
[11] Itoh T, Iwabuchi Y and Kataoka M 1988 *Phys. Status Solidi* b **145** 567
Itoh T, Iwabuchi Y and Kataoka M 1988 *Phys. Status Solidi* b **146** 531
[12] Efros Al L and Efros A L 1982 *Sov. Phys. Semicond.* **16** 772
Ekimov A I and Onushchenko A A 1982 *Sov. Phys. Semicond.* **16** 775
[13] Itoh T, Furumiya M, Ikehara T and Gourdon C 1990 *Solid State Commun.* **73** 271
[14] Banyai L, Hu Y Z, Lindberg M and Koch S W 1988 *Phys. Rev.* B **38** 8142
Yano S, Goto T and Itoh T 1996 *J. Appl. Phys.* **79** 8216
[15] Edamatsu K, Iwai S, Itoh T, Yano S and Goto T 1995 *Phys. Rev.* B **51** 11205
[16] Itoh T 1991 *Nonlinear Opt.* **1** 61
[17] Miyajima K, Oohata G, Kagotani Y, Ashida M, Edamatsu K and Itoh T 2005 *Physica* E **26** 33
[18] Yano S, Goto T, Itoh T and Kasuya A 1997 *Phys. Rev.* B **55** 1667
Yano S, Yamamoto A, Goto T and Kasuya A 1998 *Phys. Rev.* B **57** 7203
[19] Nair S V and Takagahara T 1997 *Phys. Rev.* B **55** 5153
[20] Ikezawa M and Masumoto Y 1997 *Japan. J. Appl. Phys.* **36** 4191
[21] Miyajima K, Ashida M and Itoh T 2007 *Phys. Status Solidi* b at press
[22] Gindele F, Woggon U, Langbein W, Hvam J M, Leonardi K, Hommel D and Selke H 1999 *Phys. Rev.* B **60** 8773
[23] Woggon U, Hild K, Gindele F, Langbein W, Hetterich M, Grun M and Klingshirn C 2000 *Phys. Rev.* B **61** 12632
[24] Brunner K, Abstreiter G, Bohm G, Trankle G and Weimann G 1994 *Phys. Rev. Lett.* **73** 1168
[25] Ajiki H and Cho K 2000 *Phys. Rev.* B **62** 7402
[26] Kagotani Y, Miyajima K, Oohata G, Saito S, Ashida M, Edamatsu K and Itoh T 2005 *J. Lumin.* **112** 113
[27] Oohata G, Kagotani Y, Miyajima K, Ashida M, Saito S, Edamatsu K and Itoh T 2005 *Physica* E **26** 347
[28] Eisler H J, Sundar V C, Bawendi M G, Walsh M, Smith H I and Klimov V I 2002 *Appl. Phys. Lett.* **80** 4614
[29] Malko A V, Mikhailovsky A A, Petruska M A, Hollingsworth J A, Htoon H, Bawendi M G and Klimov V I 2002 *Appl. Phys. Lett.* **81** 1303
[30] Masumoto Y, Kawamura T and Era K 1992 *Appl. Phys. Lett.* **62** 225
[31] Pavesi L, Negro L D, Mazzoleni C, Franzo G and Priolo F 2000 *Nature* **408** 440
[32] Schaller R D, Petruska M A and Klimov V I 2003 *J. Phys. Chem.* B **107** 13765
[33] Klimov V I, Mikhailovsky A A, McBranch D W, Leatherdale C A and Bawendi M G 2000 *Science* **287** 1011
[34] Miyajima K, Kagotani Y, Saito S, Ashida M and Itoh T 2006 *Phys. Status Solidi* b **243** 3795
[35] Dicke R H 1954 *Phys. Rev.* **95** 99
[36] Miyajima K, Edamatsu K and Itoh T 2004 *J. Lumin.* **108** 371
[37] Uozumi T, Kayanuma Y, Yamanaka K, Edamatsu K and Itoh T 1999 *Phys. Rev.* B **59** 9826
[38] Uozumi T and Kayanuma Y 2002 *Phys. Rev.* B **65** 165318
[39] Yamanaka K, Edamatsu K and Itoh T 2000 *J. Lumin.* **87–89** 312